CALPHAD: Computer Coupling of Phase Diagrams and Thermochemistry 34 (2010) 510–522

Contents lists available at ScienceDirect

CALPHAD: Computer Coupling of Phase Diagrams and Thermochemistry

journal homepage: www.elsevier.com/locate/calphad

The modified embedded-atom method interatomic potentials and recent progress in atomistic simulations

Byeong-Joo Lee *, Won-Seok Ko, Hyun-Kyu Kim, Eun-Ha Kim

Department of Materials Science and Engineering, Pohang University of Science and Technology (POSTECH), Pohang 790-784, Republic of Korea

ARTICLE INFO

Article history:
Received 30 August 2010
Received in revised form
14 October 2010
Accepted 14 October 2010
Available online 23 October 2010

Keywords:
Atomistic simulation
Modified embedded-atom method
Interatomic potential
Multi-scale simulation
Hybrid simulation

ABSTRACT

Atomistic simulations such as molecular dynamics and Monte Carlo are widely used for understanding the material behavior at a more fundamental level, e.g., at the atomic level. However, there still exist limitations in the variety of material systems, specimen size and simulation time. This article briefly outlines the formalism and performance of the second nearest-neighbor modified embedded-atom method, an interatomic potential formalism applicable to a wide range of materials systems. Recent progresses made to overcome the inherent size and time limitations of atomistic simulations are also introduced along with the challenges still remaining in extending their applicability. Finally, the authors release all the potential parameter sets for elements and alloy systems, and relevant homemade atomistic simulation codes based on the interatomic potential formalism with a user guide.

1. Introduction

As many of material properties are found to originate from atomic level physical factors, it is necessary to understand the material behavior from a more fundamental level, e.g., the atomic level. Today, extensive experimental and theoretical efforts are being made to understand and predict the correlation between atomic level materials' behaviors and macroscopic materials' properties. However, the atomic scale is an area still rarely accessible experimentally or by the CALPHAD approach. Atomistic computations or simulations are emerging as a useful tool for analyzing and predicting various fundamental static and dynamic properties of materials.

The most accurate theoretical method of investigating atomic level materials' properties would be to use first-principles calculations. However, due to the size (or number of atoms) limit, it is often insufficient to investigate material behaviors using only first-principles calculations. Another approach is to use (semi-)empirical interatomic potentials that can deal with more than a million atoms. It is important to note here that the interatomic potential should be able to reproduce various fundamental physical properties (structural, elastic, defect, surface, thermal properties, etc.) of relevant elements and multicomponent alloys correctly. With developments of interatomic potential formalisms that can cover a wide range of elements and alloys, the (semi-)empirical atomistic simulation on realistic materials' systems is becoming increasingly feasible.

Atomistic simulations (molecular dynamics or Monte Carlo) based on (semi-)empirical interatomic potentials can be a useful tool for analyzing and predicting defect properties, phase transformation mechanisms, kinetics and resultant structural evolutions, and dynamic behaviors of materials [1,2]. Fundamental physical quantities such as grain boundary energy, diffusivity, interactions between defects computed from atomistic simulations can also be used as input data for larger scale simulations.

Even though millions of atoms can be dealt with by empirical interatomic potentials, there still exist limitations in length and time in investigating macro-scale materials' behaviors. As a means to overcome the limitations of atomistic approaches, multi-scale simulations that combine the atomistic simulation technique with larger scale simulations have been widely attempted. A typical example of a multi-scale simulation would be to concurrently combine atomistic simulations with the continuum mechanics methods to simulate the mechanical behavior of materials [3,4]. Another multi-scale approach is the hierarchical multi-scale methods where materials' behavior occurring at different scales are simulated separately and the results at smaller scales are used as input data of more-phenomenological simulations at larger scales [5,6], as briefly mentioned above. The multi-scale simulation appears to be a promising solution to overcome length-scale problems bridging the microscopic and macroscopic modeling of materials' phenomena.

In addition to overcoming those limitations of atomistic simulations, it is necessary to extend the variety of materials' systems that can be dealt with by using (semi-)empirical

* Corresponding author. Tel.: +82 54 2792157; fax: +82 54 2792399.
E-mail address: calphad@postech.ac.kr (B.-J. Lee).

0364-5916/$ – see front matter © 2010 Elsevier Ltd. All rights reserved.
doi:10.1016/j.calphad.2010.10.007

interatomic potentials. Many empirical potential models have been proposed for various elements and alloys [7–12]. All the potential models (EAM [8], Finnis–Singlair [9], Glue [10], Tersoff [11] and RGL [12]) mentioned here are for metallic or covalent hard-materials' systems. One of them [11] is further developed in a suitable form for covalent bonding molecules and is named the reactive empirical bond-order (REBO [13]) or the adaptive intermolecular REBO (AIREBO [14]) potential. A more sophisticated potential model, the reactive force field (ReaxFF [15]), is also available and covers a wide range of materials including molecules, ceramics, metallic and ionic materials. However, the potentials for hard-materials' systems are mostly for a small group of elements. Since elements of different crystal structures have to be described using different formalisms, it is difficult to describe alloy systems consisting of elements with different structures. The modified embedded-atom method (MEAM [16]) potential is the first interatomic potential formalism that showed the possibility of describing a wide range of elements (fcc, bcc, hcp, diamond-structured and even gaseous elements) using one common formalism. The MEAM was created by Baskes [16], by modifying the EAM [8] so that the directionality of bonding is considered. The original MEAM considered interactions only among first nearest-neighbor atoms. Recently, the MEAM was modified once again by Lee and Baskes [17] and Lee et al. [18] such that the interactions among second nearest-neighbor atoms are partially considered overcoming some critical shortcomings of the original MEAM. The generalized MEAM (second nearest neighbor or 2NN MEAM) has been applied to a wide range of elements including bcc [18], fcc [19], hcp [20,21] metals, manganese [22], and diamond-structured covalent bonding elements such as carbon [23], silicon [24], germanium [25], and their alloys.

The purpose of the present article is to provide a brief review on the variety of materials' systems that have been dealt with using the 2NN MEAM interatomic potential and some recent progresses in atomistic simulations. This review presents the formalism, procedure of parameter optimization, and comparisons between the 2NN MEAM calculation and experiments or higher-level calculations for material properties of some alloy systems described using only the 2NN MEAM. We introduce some recent progresses made through efforts to overcome the inherent size and time limitation of atomistic simulations. We also describe the probable differences between the original MEAM and the present 2NN MEAM, limitations and future works necessary to extend its applicability. Finally, we release all the potential parameter sets for elements and alloy systems described by using the 2NN MEAM potential formalism, together with a homemade atomistic simulation code and its user manual, in a downloadable form.

2. Formalism and parameter optimization

The core ingredient of atomistic simulations is how to evaluate the energy of a system and interatomic forces as a function of the position of atoms. The interaction between atoms originates from electronic structures. However, in atomistic simulations, it is usually described by empirical formalisms, and the reliability of simulations is entirely dependent on the reality and accuracy of the interatomic potentials. In the MEAM, the total energy of a system is approximated as

$$E = \sum_i \left[F_i(\overline{\rho}_i) + \frac{1}{2} \sum_{j(\neq i)} S_{ij}\phi_{ij}(R_{ij}) \right] \quad (1)$$

where F_i is the embedding function, $\overline{\rho}_i$ is the background electron density at site i. S_{ij} and ϕ_{ij} (R_{ij}) are the screening factor (see Appendix) and the pair interaction between atoms i and j separated by a distance R_{ij}, respectively. For general calculations of energy, the functional forms for the two terms on the right hand side of Eq. (1), F_i and ϕ_{ij}, should be given. The background electron density at a site is computed considering directionality in bonding. A specific form is given to the embedding function F_i, but not to the pair interaction ϕ_{ij}. Instead, a reference structure where individual atoms are on the exact lattice points is defined and the total energy per atom of the reference structure is estimated from the zero-temperature universal equation of state of Rose et al. [26]. Then, the value of the pair interaction is evaluated from the known values of the total energy per atom and the embedding energy, as a function of nearest-neighbor distance. In the original MEAM [16], only first nearest-neighbor interactions are considered. The neglect of the second nearest-neighbor and more distant nearest-neighbor interactions is made effective by the use of a strong many-body screening function [27]. The consideration of the second nearest-neighbor interactions in the modified formalism (the second nearest-neighbor MEAM [17,18]) is effected by adjusting the screening parameters so that the many-body screening becomes less severe. Details of the MEAM formalism are introduced in the Appendix.

2.1. MEAM for pure elements

The original first nearest-neighbor MEAM corresponds to a special case of the more general second nearest-neighbor (2NN) MEAM. Therefore, parameter optimization is performed in the framework of the 2NN MEAM. The 2NN MEAM formalism [17,18] gives fourteen independent model parameters for pure elements: four (E_c, r_e, B, d) for the universal equation of state, seven ($\beta^{(0)}$, $\beta^{(1)}$, $\beta^{(2)}$, $\beta^{(3)}$, $t^{(1)}$, $t^{(2)}$, $t^{(3)}$) for the electron density, one (A) for the embedding function, and two ($C_{\min}$, $C_{\max}$) for many-body screening. Out of the fourteen parameters, E_c, r_e, and B are cohesive energy, nearest-neighbor distance, and bulk modulus of the reference structure, respectively. When a real structure is selected as the reference structure, these parameters become material properties, not model parameters, and the values can be obtained directly from the relevant experimental data. The d value is determined from the $(\partial B/\partial P)$ value of the reference structure. However, experimental information on $(\partial B/\partial P)$ is not always available, and first-principles calculations do not yield a good agreement with experimental information enough to assign a specific value to the d parameter for individual reference structures. The d parameter has been given either 0 or 0.05, according to $(\partial B/\partial P)$ of individual reference structures [18]. The $C_{\max}$ parameter is normally given a fixed value of 2.8. Therefore, the number of model parameters of which values should be determined is nine, A, $\beta^{(0)}$, $\beta^{(1)}$, $\beta^{(2)}$, $\beta^{(3)}$, $t^{(1)}$, $t^{(2)}$, $t^{(3)}$ and $C_{\min}$. These parameter values are usually determined by fitting static material properties such as elastic constants, vacancy formation energy, surface energy, etc. It is easy to fit a single property value exactly, but it is not always possible to fit all target property values simultaneously. Generally, the effect of each parameter on individual properties is complicated, and it is impossible to relate one property to one parameter. However, the effects of some parameters are certainly confined to only a few properties. By investigating which parameter has an effect on which property, an optimized set of parameters can be derived systematically.

Table 1 shows an example of 2NN MEAM potential parameter sets for some pure elements. It should be noted here that the unit of bulk modulus in Table 1 is different from that which appears in Eq. (A.10). The B values in Table 1 should be divided by 1.6023 to be used in Eq. (A.10).

2.2. MEAM for binary and multicomponent systems

To describe a binary alloy system, one should determine the pair interaction between different elements in addition to the descriptions for individual elements. For this, we apply a

Table 1
2NN MEAM potential parameter sets for elements, Fe, Nb, Ti, C and N.

	E_c	r_e	B	A	$\beta^{(0)}$	$\beta^{(1)}$	$\beta^{(2)}$	$\beta^{(3)}$	$t^{(1)}$	$t^{(2)}$	$t^{(3)}$	$C_{\min}$	$C_{\max}$	d
Fe[a]	4.29	2.48	1.73	0.56	4.15	1.00	1.00	1.00	2.60	1.80	−7.20	0.36	2.80	0.05
Nb[a]	7.47	2.86	1.73	0.72	5.08	1.0	2.5	1.0	1.7	2.8	−1.6	0.36	2.80	0.00
Ti[b]	4.87	2.92	1.10	0.66	2.70	1.0	3.0	1.0	6.8	−2.0	−12.0	1.00	1.44	0.00
C[c]	7.37	1.54	4.45	1.18	4.25	2.80	2.0	5.0	3.2	1.44	−4.48	1.41	2.80	0.00
N[d]	4.88	1.10	5.96*	1.80	2.75	4.00	4.0	4.0	0.05	1.00	0.0	2.00	2.80	0.00

The units of the cohesive energy E_c, equilibrium nearest-neighbor distance r_e and bulk modulus B are eV, Å, and 10^{12} dyne/cm^2, respectively. The reference structures of Fe, Nb, Ti, C and N are the bcc, bcc, hcp, diamond and dimer, respectively.
* This is an α value as defined in Eq. (A.10). Bulk modulus B is not defined for a gaseous element.
[a] Ref. [18].
[b] Ref. [20].
[c] Ref. [23].
[d] Ref. [28].

similar technique used to determine the pair interaction for pure elements. As a reference structure, we select a perfectly ordered binary intermetallic compound, where one type of atoms has only a different type of atoms as first nearest-neighbors and has only the same type of atoms as second nearest-neighbors. The Bl (NaCl type) or B2 (CsCl type) ordered structure can be a good example. For such a reference structure, the total energy per atom, E_{ij}^u (for $1/2\,i$ atom+ $1/2\,j$ atom) obtained from the universal equation of state of Rose et al. [26], is given as follows:

$$E_{ij}^u(R) = \frac{1}{2}\left[F_i(\overline{\rho}_i) + F_j(\overline{\rho}_j) + Z_1\phi_{ij}(R) + \frac{Z_2}{2}\left(S_i\phi_{ii}(aR) + S_j\phi_{jj}(aR)\right)\right] \quad (2)$$

where Z_1 and Z_2 are the numbers of first and second nearest-neighbors in the reference structure, respectively. S_i and S_j are the screening functions for the second nearest-neighbor interactions between i atoms and between j atoms, respectively, and a is the ratio between the second and first nearest-neighbor distances in the reference structure. The pair interaction between i and j can now be obtained in the following form:

$$\phi_{ij}(R) = \frac{1}{Z_1}\left[2E_{ij}^u(R) - F_i(\overline{\rho}_i) - F_j(\overline{\rho}_j) - \frac{Z_2}{2}\left(S_i\phi_{ii}(aR) + S_j\phi_{jj}(aR)\right)\right]. \quad (3)$$

The embedding functions F_i and F_j can be readily computed. The pair interactions Φ_{ii} and Φ_{jj} between the same types of atoms can also be computed from descriptions of individual elements. To obtain $E_{ij}^u(R)$, the universal equation of state, Eqs. (A.8)–(A.10), is considered once again for the binary reference structure. In this case, E_c, r_e and B correspond to the cohesive energy, equilibrium nearest-neighbor distance and bulk modulus of the binary reference structure.

As mentioned above, the extension of the MEAM to a binary alloy system involves the determination of the pair interaction between different types of atoms. The main task is to estimate the potential parameters of the universal equation of state for the reference structure. Eqs. (A.8)–(A.10) show that the potential parameters are E_c, r_e (or Ω), B and d. The first three are material properties if the reference structure is a real phase structure that exists on the phase diagram of the relevant system. Experimental data for that phase can be used directly. Otherwise, the parameter values should be optimized so that experimental information for other phases or high-level calculation results can be reproduced if available, or assumptions should be made. The fourth parameter d is a model parameter. As in the unary MEAM, the value can be determined by fitting the $(\partial B/\partial P)$ value of the reference structure. When the reference structure is not a real phase, it is difficult to estimate a reasonable value of d for the alloy system. For such alloy systems, d is given an average value of those for pure elements.

In addition to the parameters for the universal equation of state, two more model parameter groups, $C_{\min}$ and $C_{\max}$, must be determined to describe alloy systems. Each element has its own value of $C_{\min}$ and $C_{\max}$. $C_{\min}$ and $C_{\max}$ determine the extent of the screening of an atom (k) to the interaction between two neighboring atoms (i and j). For pure elements, the three atoms are all the same type (i–j–k = A–A–A or B–B–B). However, in the case of binary alloys, one of the interacting atoms and/or the screening atoms can be different types (there are four cases: i–k–j = A–B–A, B–A–B, A–A–B and A–B–B). Different $C_{\min}$ and $C_{\max}$ values may have to be given in each case. Another model parameter necessary for binary alloy systems is the atomic electron density scaling factor ρ_o (see Eq. (A.6)). For an equilibrium reference structure ($R = r_e$), the values of all atomic electron densities become ρ_o. This is an arbitrary value and does not have any effect on calculations for pure elements. This parameter is often omitted when describing the potential model for pure elements. However, for alloy systems, especially for systems where the constituent elements have different coordination numbers, the scaling factor (the ratio of the two values) has a great effect on calculations.

Examples of 2NN MEAM potential parameter sets for some binary alloy systems are shown in Table 2. As in unary parameter sets, care must be taken at the fact that the unit of bulk modulus in Table 2 is different from that which appears in Eq. (A.10).

The MEAM potential for a multicomponent alloy system is based on the MEAM for sub-unary and lower order alloy systems. As has been shown above, a binary system is described on the basis of fourteen potential parameters of each element and thirteen binary parameters. The MEAM potential for a ternary system is obtained by combining all sub-unary and binary parameters. In addition, three more ternary parameters for each of $C_{\min}(i$–k–$j)$ and $C_{\max}(i$–k–$j)$ are necessary. Generally, information on the fundamental physical properties of ternary systems is rare, and it is not easy to uniquely determine the ternary $C_{\min}(i$–k–$j)$ and $C_{\max}(i$–k–$j)$ values. In order to skip the procedure where one has to determine ternary potential parameter values without enough ternary information, some assumptions are made for the ternary $C_{\min}(i$–k–$j)$ and $C_{\max}(i$–k–$j)$ values based on binary parameters. For example, in the case of Fe–Ti–C (or N) ternary system, it is considered that two elements, Fe and Ti, are relatively similar to each other compared to interstitial atoms such as C or N. It is assumed that the degree of screening by a C atom to the interaction between Fe and Ti atoms [$C_{\min}$ and $C_{\max}$(Fe–C–Ti)] is an average between those to the Fe–Fe [$C_{\min}$ and $C_{\max}$(Fe–C–Fe)] and Ti–Ti [$C_{\min}$ and $C_{\max}$(Ti–C–Ti)] interactions. Similarly, the degree of screening by an Fe (or Ti) atom to the interaction between Ti (or Fe) and C atoms [$C_{\min}$ and $C_{\max}$ (Ti–Fe–C) or $C_{\min}$ and $C_{\max}$ (Fe–Ti–C)] is assumed to be an average between

Table 2
2NN MEAM potential parameter sets for the binary M–X (M = Fe, Ti and X = C, N) and Fe–Ti systems [29].

	Fe–C [30]	Fe–N [28]	Ti–C [31]	Ti–N [31]	Fe–Ti [32]
E_C	$0.75E_c^{Fe} + 0.25E_c^{C} + 0.95$	$0.5E_c^{Fe} + 0.5E_c^{N} + 0.7$	$0.5E_c^{Ti} + 0.5E_c^{C} - 0.78$	$0.5E_c^{Ti} + 0.5E_c^{N} - 1.74$	$0.5E_c^{Fe} + 0.5E_c^{Ti} - 0.22$
r_e	2.364	2.09	2.210	2.121	2.58
B	2.644	2.195	2.419	3.200	1.89
d	$0.75d^{Fe} + 0.25d^{C}$	$0.5d^{Fe} + 0.5d^{N}$	$0.5d^{Ti} + 0.5d^{C}$	$0.5d^{Ti} + 0.5d^{N}$	$0.5d^{Fe} + 0.5d^{Ti}$
C_{min}(M–X–M)	$0.36(=C_{min}^{Fe-Fe-Fe})$	0.16	0.64	0.16	1.21
C_{min}(X–M–X)	0.16	0.16	0.64	0.09	0.78
C_{min}(M–M–X)	0.16	0.16	$[0.5(C_{min}^{Ti})^{1/2} + 0.5(C_{min}^{C})^{1/2}]^2$	0.81	$[0.5(C_{min}^{Fe})^{1/2} + 0.5(C_{min}^{Ti})^{1/2}]^2$
C_{min}(M–X–X)	0.16	$[0.5(C_{min}^{Fe})^{1/2} + 0.5(C_{min}^{N})^{1/2}]^2$	$[0.5(C_{min}^{Ti})^{1/2} + 0.5(C_{min}^{C})^{1/2}]^2$	$[0.5(C_{min}^{Ti})^{1/2} + 0.5(C_{min}^{N})^{1/2}]^2$	$[0.5(C_{min}^{Fe})^{1/2} + 0.5(C_{min}^{Ti})^{1/2}]^2$
C_{max}(M–X–M)	2.80	1.44	$1.44(=C_{max}^{Ti})$	2.80	$2.80(=C_{max}^{Fe})$
C_{max}(X–M–X)	1.44	2.80	$2.80(=C_{max}^{C})$	$2.80(=C_{max}^{N})$	2.80
C_{max}(M–M–X)	2.80	2.80	2.80	1.44	2.80
C_{max}(M–X–X)	2.80	2.80	2.80	2.80	2.80
ρ_0	$\rho_0^{C}/\rho_0^{Fe} = 6.0$	$\rho_0^{N}/\rho_0^{Fe} = 18$	$\rho_0^{C}/\rho_0^{Ti} = 6.0$	$\rho_0^{N}/\rho_0^{Ti} = 18$	$\rho_0^{Ti}/\rho_0^{Fe} = 1.0$

The units of the cohesive energy E_c, the equilibrium nearest-neighbor distance r_e and the bulk modulus B are eV, Å and 10^{12} dyne cm^{-2}, respectively.
The reference structures of Fe–C, Fe–N, Ti–C, Ti–N, and Fe–Ti are the $L1_2$-Fe_3C, NaCl-type (B1) FeN, TiC, TiN and CsCl-type (B2) FeTi, respectively.

Table 3
Parameter sets of C_{max} and C_{min} for Fe–Ti–X (X = C, N) ternary systems determined from constituent binary parameters [29].

	Type	Default assumption
C_{max}	C (Fe–X–Ti)	$[0.5(C^{Fe-X-Fe})^{1/2} + 0.5(C^{Ti-X-Ti})^{1/2}]^2$
	C (Fe–Ti–X)	$[0.5(C^{Fe-Fe-X})^{1/2} + 0.5(C^{Ti-Ti-X})^{1/2}]^2$
	C (Ti–Fe–X)	$[0.5(C^{Fe-Fe-X})^{1/2} + 0.5(C^{Ti-Ti-X})^{1/2}]^2$
C_{min}	C (Fe–X–Ti)	$[0.5(C^{Fe-X-Fe})^{1/2} + 0.5(C^{Ti-X-Ti})^{1/2}]^2$
	C (Fe–Ti–X)	$[0.5(C^{Fe-Fe-X})^{1/2} + 0.5(C^{Ti-Ti-X})^{1/2}]^2$
	C (Ti–Fe–X)	$[0.5(C^{Fe-Fe-X})^{1/2} + 0.5(C^{Ti-Ti-X})^{1/2}]^2$

those by an Fe atom to the Fe–C [C_{min} and C_{max} (Fe–Fe–C)] and by a Ti atom to the Ti–C [C_{min} and C_{max} (Ti–Ti–C)] interactions. These assumptions have been introduced to the MEAM potential of Fe–Ti–C, Fe–Ti–N [29], Fe–Nb–C and Fe–Nb–N [33] ternary systems, and have been found to result in reasonable descriptions of interfacial properties between Fe matrix and TiC, NbC carbides or TiN, NbN nitrides. They are now adapted as a first approximation to estimate the ternary $C_{min}(i–k–j)$ and $C_{max}(i–k–j)$ parameter values when decisive information on ternary properties is not available. As an example, Table 3 shows the ternary C_{min} and C_{max} parameters of the Fe–Ti–C system, automatically determined from parameters of constituent binary systems. For quaternary or higher order systems, the (2NN) MEAM needs no more parameters other than the constituent unary, binary and ternary parameters.

3. Variety of material systems dealt with by the 2NN MEAM

As already mentioned, the original modified embedded-atom method (MEAM) potential created by Baskes [16] showed the possibility for the first time that a single potential formalism can reproduce physical properties of many elements with various crystal structures including hcp, diamond cubic as well as fcc and bcc. However, when applied to an atomistic simulation on some bcc metals, the MEAM revealed that it has critical problems. First, for many bcc metals, the surface energy of the {111} surface was computed to be smaller than that of the {100} surface, which was contrary to experimental fact [34,35]. Second, more critically, a structure more stable than the bcc was created during a molecular dynamics simulation at finite temperatures for some bcc elements (Fe, Cr, Mo, …) [17,18]. Simple changes of model parameters could not solve those problems. The original MEAM was formulated to consider only first nearest-neighbor interactions by using a strong screening function. However, the second nearest-neighbor distance is larger than the first nearest-neighbor distance by only about 15% in bcc structures, and the second nearest-neighbor interactions might not be wholly negligible.

Much effort was devoted to find a way to solve the above-mentioned problems, considering up to second or even third nearest-neighbor interactions. Finally, it was found that the above-mentioned problems in the original MEAM for bcc metals could be solved when considering partially the second nearest-neighbor interactions as well as the first nearest-neighbor interactions [17,18]. Later, it was found that some structural stability problems also arise in fcc and hcp MEAM, and that those problems could also be solved by adjusting the degree of many-body screening as has been done for the bcc elements. The second nearest-neighbor (2NN) MEAM formalism thus created has been applied to a wide range of elements and alloy systems. Table 4 shows a list of material systems where the author's group has developed a 2NN MEAM interatomic potential during the last decade. Here, the material systems denoted with an asterisk (∗) are those where the present 2NN MEAM is a unique interatomic potential ever published for the system.

As an example, some comparisons between the 2NN MEAM calculations and experiments or higher-level calculations will be made in this section, for some fundamental physical properties of the Fe–N, Ti (or Nb)–C(or N) binary and Fe–Ti(or Nb)–C(or N) ternary systems. Table 5 shows physical properties of nitrogen in bcc and fcc Fe–N alloys, in comparison with experimental data or higher-level calculations. Corresponding 2NN MEAM values of carbon are also presented for comparison. The dilute heat of solution, migration energy barrier and binding properties between a nitrogen atom and other primary defects are reasonably reproduced for both bcc and fcc Fe–N alloys. Especially, for the fcc Fe alloys, it is experimentally known that two neighboring nitrogen atoms and two carbons atoms are both weakly repulsive to each other (with negative binding energies) in the Fe–N and Fe–C fcc alloys, respectively [51]. Furthermore, the two nitrogen atoms occupying the second nearest-neighboring interstitial sites (⟨100⟩ alignment) are known to be less repulsive to each other than those occupying the first nearest-neighboring interstitial sites (⟨110⟩ alignment), and the opposite occurs in the case of two neighboring carbon atoms [51]. The present Fe–N and Fe–C potentials [28,30] can reproduce the above experimental behavior of nitrogen and carbon atoms in fcc Fe correctly, at least qualitatively. It should be mentioned here that the 2NN MEAM also describes the fundamental physical property of fcc Fe with an acceptable accuracy, even though the phase transition between bcc and fcc Fe is not reproduced.

The development of the Ti(or Nb)–C(or N) binary and Fe–Ti(or Nb)–C(or N) ternary interatomic potentials can be counted as one of the most successful achievements of the 2NN MEAM study. As shown in Tables 6–9, the potentials reproduce lattice constant, enthalpy of formation, elastic properties, surface energy

Table 4
Materials' systems where a (2NN) MEAM interatomic potential was developed by the present author's group.

Pure elements	Fe, Cr, Mo, W, V, Nb, Ta [18] Cu, Ag, Au, Ni, Pd, Pt, Al, Pb [19] Ti, Zr [20], Mg [21] Mn* [22] C [23], Si [24], Ge [25] In* [36], Sn [37]
Carbide system	Fe–C [30], Ti–C* [31], Nb–C* [33], Mo–C* [37], W–C* [37] Fe–Ti–C* [29], Fe–Nb–C* [33], Fe–Mo–C* [37], Fe–W–C* [37]
Nitride system	Fe–N* [28], Ti–N* [31], Nb–N* [33], Al–N* [37] Fe–Ti–N* [29], Fe–Nb–N* [33], Fe–Al–N* [37]
Hydride system	Fe–H [38], V–H* [39], Al–H* [37], Ni–H [37]
Fe-binary system	Fe–Al [40], Fe–Cr [41], Fe–Cu [42], Fe–Mn* [22], Fe–Mo [37], Fe–Nb [32], Fe–Pt [43], Fe–Sn* [37], Fe–Ti [32], Fe–W [37]
Metallic binary system	Ag–Cu [44], Ag–Zr [44], Al–Mg [21], Al–Ni [45], Al–V [37] Cu–Ni [46], Cu–Ti [47], Cu–Zr [48], Ni–V [37], Ni–W [49]
Metallic ternary system	Cu–Zr–Ag [44]
Semiconducting system	Ga–N [50], In–N [50], Ga–In* [50], Ga–In–N [50]

Table 5
Physical properties of nitrogen in bcc and fcc Fe–N alloys calculated using the 2NN MEAM potential [28], in comparison with experimental data or other calculations, and with corresponding calculated properties of carbon in Fe. a_o is the equilibrium lattice constant, and the crystallographic directions ⟨111⟩, etc., represent the direction of nitrogen-nitrogen alignment (see text). The reference states of all bindings are the states where all the individual defects are separated and non-interacting with each other.

In BCC Fe	MEAM	Expt./calc.[a]	Corresponding 2NN MEAM value for carbon [Ref. [30]]
Dilute heat of solution of nitrogen (eV)	0.33	0.32	1.22
Migration energy barrier of nitrogen (eV)	0.78	0.76, 0.80	0.82
Vacancy-nitrogen binding energy (eV)	0.64	0.67, 0.71	0.90
Nitrogen–nitrogen binding energy (eV)	0.06 ⟨111⟩	−0.12, −0.03	0.34 ⟨120⟩
	0.06 ⟨120⟩	−0.28, −0.16	0.32 ⟨100⟩
		0.07	
Self interstitial-nitrogen binding energy (eV)	0.45	−0.35, −0.18	0.68
Vacancy-two nitrogen binding energy (eV)	0.71 ⟨100⟩	1.25, 1.54	1.86 ⟨100⟩
In FCC Fe			
Dilute heat of solution of nitrogen (eV)	−0.48	−0.53	0.30
Migration energy barrier of nitrogen (eV)	1.36	1.75	1.52
Vacancy- nitrogen binding energy (eV)	0.23	–	0.67
Nitrogen–nitrogen binding energy (eV)	−0.10 ⟨100⟩	–	−0.12 ⟨110⟩
	−0.31 ⟨110⟩	–	−0.35 ⟨100⟩
Self interstitial-nitrogen binding energy (eV)	0.20	–	0.58
Vacancy-two nitrogen binding energy (eV)	0.38 ⟨100⟩	–	1.55

[a] Ref. [28] and references therein.

Table 6
Lattice parameter and enthalpy of formation of TiC, TiN, NbC and NbN carbides or nitrides calculated using the 2NN MEAM potentials [31,33], in comparison with experimental data and/or first-principles calculations.

	Lattice constant, a (Å)		Enthalpy of formation (eV/atom)	
	MEAM	Expt.	MEAM	Expt.
TiC	4.420	4.317–4.330[a]	−0.78	−0.78[a]
TiN	4.242	4.240–4.430[a]	−1.74	−1.74[a]
NbC	4.560	4.469–4.471[b]	−0.730	−0.701 to −0.731[b]
NbN	4.395	4.379–4.394[b]	−1.23	−1.175 to −1.233[b]

The reference states for the enthalpy of formation are hcp Ti, bcc Nb, graphite C and gaseous N_2 at 1 atm.
[a] Ref. [31] and references therein.
[b] Ref. [33] and references therein.

of the NaCl type TiC, TiN, NbC and NbN carbides or nitrides, and interfacial energy between those compounds and the bcc Fe matrix in a reasonable agreement with experimental information or higher-level calculations. This means that one can investigate the nucleation kinetics of those important precipitates in steels more quantitatively. Since the 2NN MEAM potential for carbon can well describe the fundamental physical properties of graphene and carbon nanotubes [23], we expect that one can also use the present potentials for carbide systems for an atomistic study of the interaction between graphene or carbon nanotubes and metallic elements.

4. Recent progress in atomistic simulations

The inherent limitations in length and time should be overcome in order to maximize the applicability of atomistic simulations to the fundamental study of the dynamic properties of structural materials. Currently, a multi-scale simulation scheme that combines the grain boundary property database and the mesoscale simulation technique such as the phase field method is being attempted to predict microstructure evolution in polycrystalline materials more realistically. A hybrid simulation scheme that combines the molecular dynamics, Monte Carlo and molecular static simulation techniques is also being attempted as a means to overcome the time limitation of molecular dynamics simulations. In this section, we will briefly introduce the motivation and basic idea of the above-mentioned multi-scale and hybrid simulation with some preliminary results.

4.1. A multi-scale simulation to overcome the size limitation

Even though atomistic simulations on the morphological evolution of nano-grained (of a few nanometers size) polycrystalline materials have been performed [52], one should accept for the moment that the microstructural evolution of micro-scale polycrystalline materials is not an area for atomistic approaches. Instead, mesoscale simulations based on the phase field method or Monte Carlo are widely used for the prediction of microstructural evolution. Fig. 1a, b show snapshots of a phase field method simulation [53] for a phase transformation from austenite (γ) to ferrite (α) in a steel. The pink (or white grey) grains are ferrite grains that grow at the expense of yellow (or white) austenite grains. The initial microstructure, material composition (Fe-0.5%Mn-0.1%C) and cooling rate (1 °C/s) are exactly the same for the two cases. However, the growth morphology of the ferrite is certainly different from each other. The transformation kinetics is also different in the two cases. The reason for the difference in the microstructural evolution and transformation kinetics is the wetting angle (36° vs. 120°) of ferrite grains at triple junctions with two

Table 7
Elastic properties of TiC and TiN calculated using the present (2NN) MEAM potentials, in comparison with experimental data and first-principles calculations [31,33].

	B		C_{11}		C_{12}		C_{44}	
	MEAM	Expt.	MEAM	Expt.	MEAM	Expt.	MEAM	Expt.
TiC	2.42	2.41, 2.42[a]	5.22	5.00, 5.13[a]	1.02	1.13, 1.06[a]	1.29	1.75, 1.78[a]
TiN	3.2	3.20, 2.92[a]	6.59	6.25[a]	1.50	1.65[a]	1.83	1.63[a]
NbC	3.40	2.96–3.40[b]	5.49	6.20[b]	2.35	2.00[b]	1.73	1.50[b]
NbN	3.54	2.92, 3.20[b]	5.79	6.08, 5.56[b]	2.42	1.34, 1.52[b]	1.68	1.17, 1.25[b]

The units of elastic constants B, C_{11}, C_{12}, C_{44} are 10^{12} dyne/cm^2.
[a] Ref. [31] and references therein.
[b] Ref. [33] and references therein.

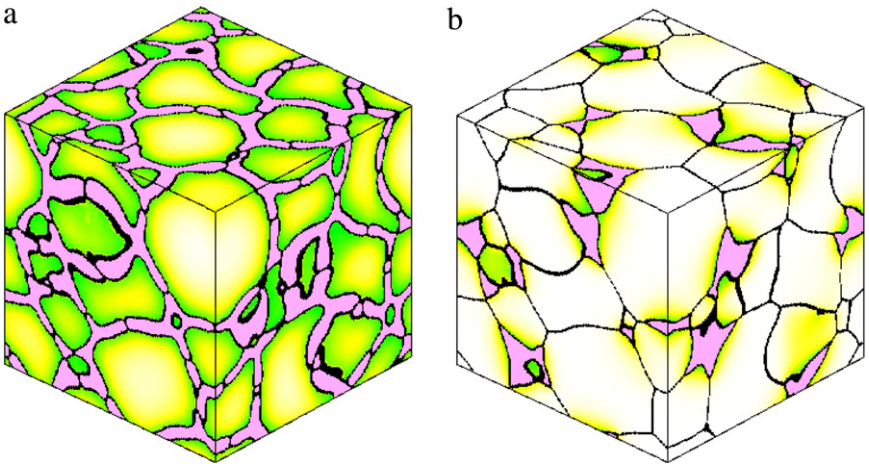

Fig. 1. Snapshots of a phase field method simulation for a phase transformation from austenite (γ) to ferrite (α) in a steel (Fe-0.5%Mn-0.1%C) under the same cooling rate (1 °C/s]) but with different wetting angle, (a) 36° and (b) 120°, of ferrite grains at triple junctions [53]. The pink (or white grey) grains are ferrite grains that grow at the expense of yellow (or white) austenite grains. (For interpretation of the references to colour in this figure legend, the reader is referred to the web version of this article.)

Table 8
Relaxed surface energy of low index surfaces of TiC, TiN, NbC and NbC carbides or nitrides calculated using the 2NN MEAM potentials [31,33], in comparison with first-principles calculations.

	Surface	MEAM	First principles calculations[a]		Surface	MEAM	First principles calculations[b]
TiC				NbC			
	(100)	2.910	1.665–2.254, 2.73*		(100)	2.46	2.81
	(110)	3.764	3.631–3.78		(110)	2.65	–
	(111)	4.048	3.122–5.63		(111)	2.47	–
TiN				NbN			
	(100)	1.301	1.06–1.38, 1.98*		(100)	1.36	1.13
	(110)	2.462	2.59–2.86, 4.06*		(110)	1.90	2.12
	(111)	3.652	3.62–4.95		(111)	2.26	2.04–2.15

The unit of the surface energy is J/m2. Values marked with a "* " are unknown whether they are relaxed values or not.
[a] Ref. [31] and references therein.
[b] Ref. [33] and references therein.

Table 9
Calculated coherent interfacial energy between bcc Fe and TiC, TiN, NbC or NbN with a Baker–Nutting orientation relationship, in comparison with first-principles calculations and literature data [29,33].

Interface	MEAM	First principles calculation	Other estimation
Fe/TiC	0.302	0.263[a]	–
Fe/TiN	0.175	0.343[a]	–
Fe/NbC	0.817	−0.17[b]	0.3–1.0[b]
Fe/NbN	0.245	−0.23[b]	0.23[b]

The unit of the interfacial energy is J/m^2.
[a] Ref. [29] and references therein.
[b] Ref. [33] and references therein.

austenite grains, which is given externally as an input data. The wetting angle is determined by the relative size of γ/α interfacial energy and γ/γ grain boundary energy. This means that the grain boundary energy and interfacial energy play a decisive role in the microstructural evolution and transformation kinetics. However, the grain boundary energy and interfacial energy, especially their variation depending on the type of grain boundary or interface is very difficult to measure experimentally. The basic idea of the present multi-scale simulation is to calculate the grain boundary or interfacial energy using an atomistic computation, construct a database and implement it in mesoscale simulation techniques.

Fig. 2 shows part of the databases for α/α, γ/γ grain boundary and γ/α interfacial energy of Fe in a specially designed order. Before the construction of such databases, one needs to clarify two issues. One is how to identify a specific grain boundary as a function of five degrees of freedom (three from misorientation and two from inclination) among the infinite number of probable grain boundaries with arbitrary misorientation and inclination angles. The other is how to calculate the grain boundary energy of a large number of grains within a reasonable time. In order to clarify the first issue, an identification scheme of grain boundaries based on the misorientation and inclination was developed, and the details will be reported separately [54]. The grain boundaries in Fig. 2 can be divided into several groups, where the grain boundaries in each group have the same misorientation but different inclination angles.

Normally, the computation of grain boundary energy is made by comparing the energies of two samples, one with a grain boundary between two single crystals under a given misorientation and inclination, and the other without the grain boundary. The easiest way to make this comparison is to make the sample with the grain boundary have no other grain boundary or free surface, and compare the energy with the ideal bulk energy of a single crystal of the same material. The sample with only one type of grain boundary and no other grain boundary or free surface can be made by assigning a three-dimensional periodic boundary condition to the sample. However, it is generally impossible to assign a three-dimensional periodic boundary condition to a sample made by combining two crystals under an arbitrary misorientation and inclination. This is because the sample dimension of each crystal into a direction parallel to the boundary where a periodic boundary condition is assigned, does not match each other. In this method, the sample size should be determined carefully to be able to apply the periodic boundary condition into all planar directions, and the resultant sample size is different in all individual samples with difference misorientation. A new method proposed [55] to overcome the above mentioned difficulty is to use a spherical sample. Fig. 3 shows the outline of the method. First, two identical

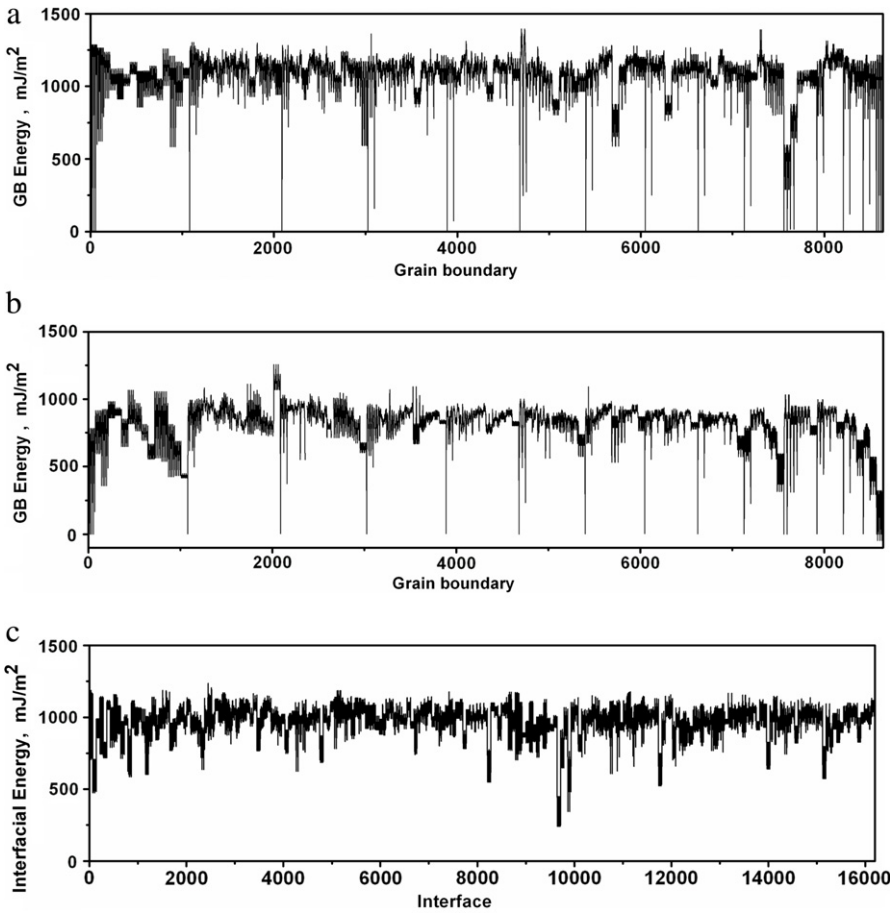

Fig. 2. (a) α/α, (b) γ/γ grain boundary and (c) γ/α interfacial energy of Fe for selected grain boundaries and interfaces.

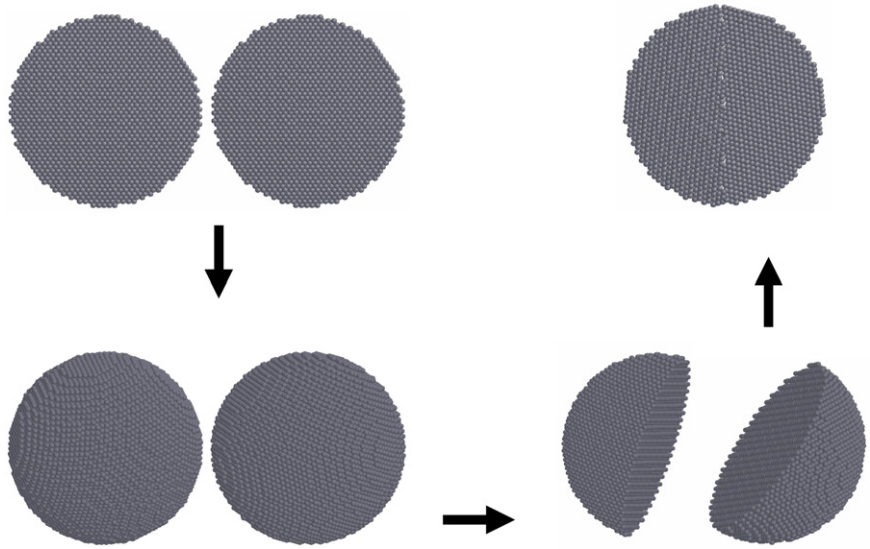

Fig. 3. A scheme for the computation of grain boundary energy under an arbitrary misorientation and inclination angle [55].

spherical samples are prepared and each sample is rotated so that the two samples have a predetermined misorientation. Then, each spherical sample is cut into two parts with exactly the same size, in a direction of a predetermined inclination angle. Finally, the half spheres from each sample are combined to make a new sphere that involves a newly created grain boundary under a given misorientation and inclination. Since the difference in the potential energy between the original and the newly created sphere should come from the newly created grain boundary in the new sphere, the grain boundary energy (energy per area) can always be computed for arbitrary misorientation and inclination angles. An advantage of this method is that the procedure for computing the grain boundary energy for a series of different grain boundaries can be fully computerized because one does not need to adjust the sample size of each sample to apply the three-dimensional periodic boundary condition. This is the reason why

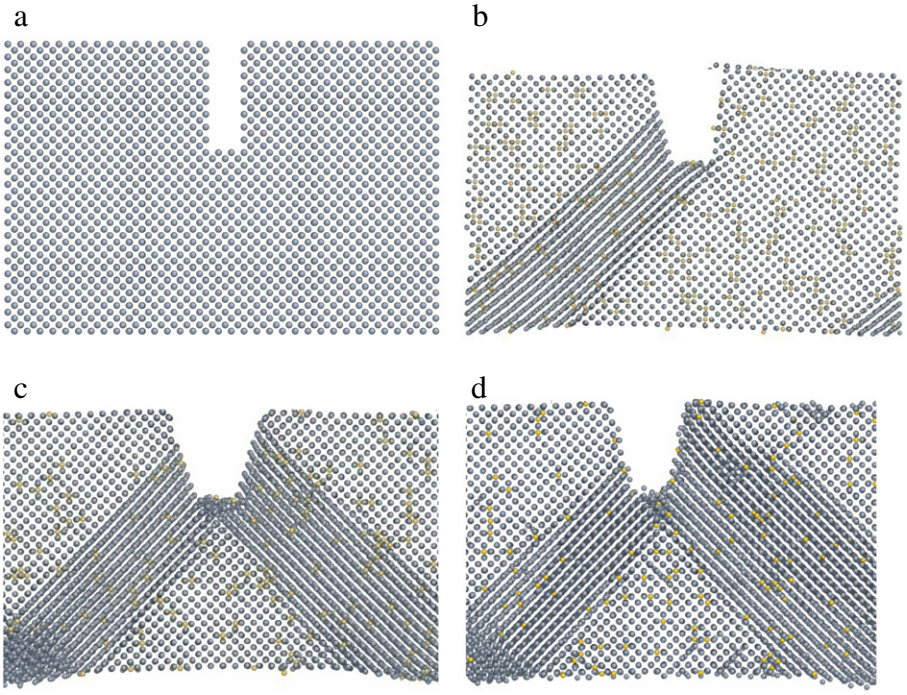

Fig. 4. A molecular dynamics simulation for tensile loading. (a) Initial sample for pure bcc Fe and binary bcc alloy samples with randomly distributed (b) 0.8 at.% H, (c) 0.8 at.% C and (d) 0.8 at.% N interstitial atoms, extended to about 10 % along the ⟨100⟩ direction at 100 K.

the energy of a large number of grain boundaries or interfaces can be calculated as shown in Fig. 2, within a practically reasonable time.

An effort is now being made to implement the grain boundary and interfacial energy databases to a phase field simulation technique.

4.2. A hybrid simulation to overcome the time limitation

The MD simulation has been widely used to investigate the dynamic behavior of materials during phase transformations or deformations. However, the time duration that can be covered by MD simulations is normally in the order of nano-seconds at most. In order to observe any dynamic responses of materials during phase transformations or deformations, a certain amount of thermodynamic or mechanical driving force needs to be applied. Introduction of a certain amount of driving force for short simulation time results in an unrealistically high cooling rate or strain rate. In addition to the unrealistically high driving forces, an inherent problem of the MD simulations due to the short simulation time is that the effect of alloying elements on the transformation or deformation behavior of materials cannot be examined correctly. This is because the short simulation time cannot allow the probable diffusion of alloying elements towards or away from the defects (grain boundaries, crack tip, etc.). As a means to overcome the limitation of MD simulation due to the short simulation time, one can think of a kinetic MC simulation or a hybridization of the MD and MC techniques.

Fig. 4 shows some tensile loading simulation results that motivated the development of a new approach to overcome the time limitation of MD technique. An attempt was made to investigate the effect of hydrogen, carbon or nitrogen interstitial atoms on the tensile behavior of bcc Fe using an MD simulation. Fig. 4(a) shows the initial bcc Fe sample of a size of $10.1 \times 6.8 \times 4.2$ nm^3 with about 23,000 Fe atoms. Fig. 4(b)–(d) show binary alloy samples with randomly distributed 0.8 at.% H, 0.8 at.% C or 0.8 at.% N interstitial atoms, extended to about 10 % along the ⟨100⟩ direction at 100 K. Here, the tensile elongation is made by extending the sample dimension along the loading direction by 1%, running a series of MD runs (equilibration), and repeating the extension and the MD equilibration. Under this condition of simulation, pure Fe samples show a ductile plastic deformation. Even though the effect of carbon or nitrogen on the tensile behavior of Fe is not clearly known, the hydrogen embrittlement is a well known experimental fact. Therefore, it was expected that some different tensile behavior would be observed at least for the Fe–H alloy sample. However, as shown in Fig. 4(b)–(d), all alloy samples showed a plastic deformation similar to the pure Fe sample.

Interstitial atoms such as H, C or N have a significant effect on the mechanical property of Fe even with a small addition. A typical example is the hydrogen embrittlement as already mentioned. This is believed to originate from the strong interaction of hydrogen atoms with defects such as interfaces, dislocations as well as crack tips. However, because of being incapable of allowing the diffusion of hydrogen atoms due to the short simulation time, the strong interactions between hydrogen atoms and defects, and their probable effects on the tensile behavior can not be realized during the MD simulation. As a means to observe the effect of hydrogen atoms on tensile behavior, a large amount of hydrogen atoms (more than 10 at.%) was arbitrarily precharged in front of the crack tip, in a previous study [56]. In the present study, instead of using the precharged high contents of alloying elements in front of the crack tip, a Monte Carlo change of interstitial atom positions is inserted between a series of MD runs. In the MC simulation, an interstitial atom and one of its nearest neighboring interstitial sites are randomly selected, and the position of the selected interstitial atom is changed to the selected nearest neighboring interstitial site. The acceptance of the MC attempt (change of atom position) is decided by comparing the energy before and after the MC attempt.

Allowing modification of atomic positions by inserting the MC routine between MD runs can be regarded as a solution to overcome the above-mentioned time limitation of MD simulations. However, in the case of interstitial alloys, because of the strong lattice strain around the interstitial atoms, simple changes in the atomic position of an interstitial atom to the neighboring interstitial site cause a significant increase of energy. Those changes

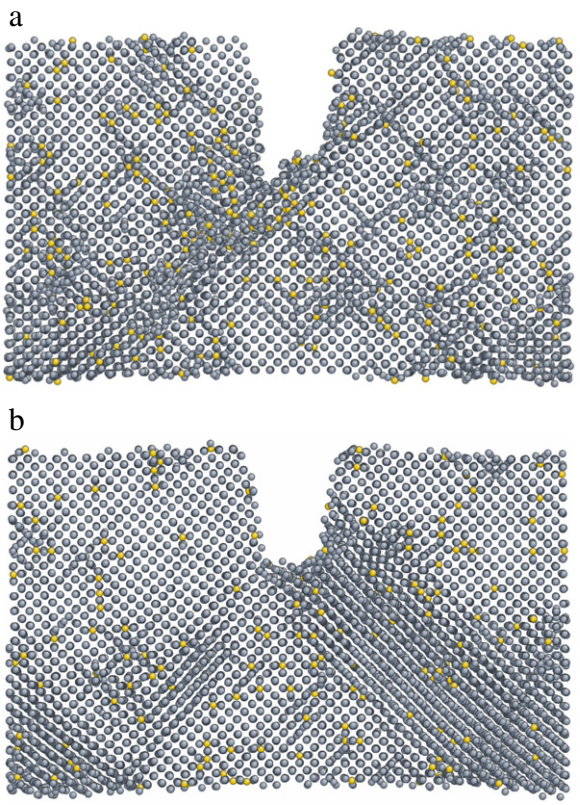

Fig. 5. A molecular dynamics + Monte Carlo + molecular statics hybrid simulation for tensile loading, for binary bcc (a) Fe-0.8 at.% C and (b) Fe-0.8 at.% N alloys at 100 K.

are never accomplished during ordinary MC simulations. This means that even a simple diffusion of a solute atom cannot be realized by the MC simulation when the solution of the solute atom causes a large local strain on surrounding atoms. This problem is solved by introducing a molecular statics (MS) relaxation process just after individual MC attempts. This new hybrid approach was applied to the tensile simulation problems as shown in Fig. 4. Preliminary results for the effect of carbon and nitrogen atoms on the tensile behavior of bcc Fe are shown in Fig. 5. The positions of C and N atoms were initially the same. Mutual differences between C and N atoms in the redistribution around the crack tip and in the effect on the crack propagation behavior are shown, even though further tests with longer simulation time and with different loading directions are necessary to draw a clear conclusion.

This MD + MC + MS hybrid simulation technique can be generally applied to a wide range of multicomponent crystalline materials systems as well as the above-mentioned interstitial alloy systems to investigate the effects of solute atoms on atom-level structural behaviors. We propose this MD + MC + MS hybrid simulation technique as a means to overcome the inherent time limitation of MD simulations.

5. Challenges and opportunities

As mentioned earlier, the second nearest neighbor (2NN) MEAM interatomic potential formalism is applicable to a wider range of materials. The hierarchical multi-scale simulations and a hybrid simulation that combines a molecular dynamics technique with a Monte Carlo accompanied by a molecular statics relaxation have been proposed as a means to overcome the inherent limitations in length and time of atomistic simulations. Even with the above-mentioned progress, there are many points that need further improvements to extend the applicability of atomistic approaches to materials research. We describe some of those points in this section.

5.1. Differences between the original and 2NN MEAM

Once the potentials are verified to reproduce target material properties, they are widely employed in simulations of dynamic systems in which the local environment deviates significantly from the equilibrium, i.e., the reference crystal structure. However, reproduction of equilibrium properties does not necessarily guarantee that the potential is able to accurately describe physical phenomena under conditions different from those it was designed for, which is known as transferability. The extension of transferability of empirical potentials is still a challenging problem.

A great amount of research has been carried out to develop interatomic potentials with a good transferability for various material systems based on the (2NN) MEAM formalism. In a situation where the availability of interatomic potentials with a good transferability still limits the applicability of atomistic simulations, developing potentials based on the separate formalisms (the original MEAM vs. 2NN MEAM) may reduce the efficiency of research efforts. It is necessary to combine the potential parameters based on the two MEAM formalisms into a single potential database. For this purpose, one needs to be aware of the basic requirements of interatomic potentials and probable differences between the two MEAM formalisms.

Many of the bcc, fcc and hcp elements have two versions of MEAM potential parameter sets, one based on the original MEAM [16,57] and the other based on the 2NN MEAM [18–21]. Since the original MEAM corresponds to a special case where all the second nearest-neighbor interactions are fully screened by nearest-neighbor atoms, all the original MEAM parameter sets for pure elements can be essentially used within the framework of the 2NN MEAM. However, one needs to check two points. First, the original MEAM parameters are optimized mainly considering 0 K static properties. Even though the calculated 0 K properties may appear to be in good agreement with experiments or higher-level calculations, there can be a structural change to an unidentified crystal structure during finite temperature MD runs. Actually, this was one of the main reasons for the creation of the 2NN MEAM formalism. Therefore, when using an original MEAM potential for pure elements, it is strongly recommended to check if the equilibrium structure is maintained at finite temperatures up to melting. Second, as mentioned in the Appendix, the way of combining the partial electron densities to give the total background electron density is not unique, and several expressions have been proposed [27]. The expression used in the 2NN MEAM is the Eq. (A.4), and it is different from that used in the original MEAM. This difference can have an effect on the planar defect properties such as surface energy or stacking fault energy. Therefore, one should check the probable differences in the calculated planar properties when using an original MEAM parameter set in a code based on the 2NN MEAM and vice versa. In the case of alloy systems, both formalisms use different values of $t()$ parameters when computing total background electron density using Eq. (A.5). The 2NN MEAM uses values for the element on each atomic site while the original MEAM uses a kind of average values. Because of this, unfortunately, the alloy parameter sets are not transferable between the two formalisms.

5.2. Toward an enrichment of MEAM potential database

Currently, the material systems covered by the 2NN MEAM are mainly metallic and covalent bonding hard-material systems. However, ionic bonding materials, the oxides, are the subject of increasingly extensive research for functional materials and provide opportunities of atomistic investigation. Even though

interatomic potential models suitable for oxides are already available [58–61], those potential models also need an extension to a wider range of material systems. In order to be able to investigate metal/oxide interfaces, for example, an interatomic potential formalism that can deal with both metallic and ionic systems simultaneously would be highly required. The MEAM has been applied also to oxide systems. The fundamental physical properties such as atomic structure, cohesive energy, lattice parameter and elastic constants are reproduced in fair agreement with experimental data for Al_2O_3 [62], for example. However, the MEAM for oxide systems does not consider the electrostatic Coulomb force, and the effect of not considering the essential electrostatic term on the transferability of the potential is unknown. In any case, without the electrostatic term which is central for ionic systems, the MEAM approach cannot be thought to be mimicking nature correctly, and it is recommended to develop a new potential model introducing the electrostatic term to the current (2NN) MEAM formalism.

One more materials property that the current (2NN) MEAM (also all the other empirical potential models) needs to introduce is the magnetic ordering. Currently, one cannot investigate materials phenomena that originate from the magnetic ordering transition including the bcc/fcc transition in pure Fe, using (semi-)empirical atomistic approaches. The authors are aware of the recent effort to include the magnetic contribution in interatomic potential [63] and to reproduce the bcc/fcc transition in pure Fe without considering the magnetic term [64], both of which can be a good starting point to give a remedy for the problem of magnetic ordering and its probable effects.

As mentioned earlier, the (2NN) MEAM interatomic potential formalism needs to be further extended to be applicable to oxide systems as well as the metallic and semiconducting material systems and to consider the magnetic contributions as well. Even with the limitations, the 2NN MEAM already covers a wide range of material systems, and it is being applied to multi-scale and hybrid simulations to overcome the inherent size and time limitations of atomistic simulations. As a means to extend and promote applications of this atomistic materials research technique, the authors release the source code of atomistic simulation based on the 2NN MEAM formalism together with a potential database and a user guide of the program, in the form of supplementary materials (see the online version at doi:10.1016/j.calphad.2010.10.007) of the present article. Any update of the software and database will be available on the website: http://cmse.postech.ac.kr.

6. Conclusion

The implementation of a grain boundary energy database obtained from an atomistic calculation on mesoscale simulation techniques is proposed as a new class of hierarchical multi-scale simulations to overcome the inherent size limitation of atomistic simulations. In addition, we propose the hybrid simulation that combines a molecular dynamics with a Monte Carlo change of atomic positions accompanied by a molecular statics relaxation as a means to overcome the inherent time limitation of atomistic simulations. Even though there are many points that limit wider applications and need further improvements, the 2NN MEAM is an interatomic potential formalism that can deal with a wide range of material systems. We hope that the proposed multi-scale and hybrid simulation techniques and the relevant software and database released with the present article may enhance the atomistic materials research.

Acknowledgements

This work has been financially supported by a grant from the Fundamental R&D Program for Core Technology of Materials funded by the Ministry of Knowledge Economy, Korea and the Pohang Steel Company (POSCO).

Appendix

The formalism of the (2NN) MEAM for pure elements is now presented. It has been shown in Eq. (1) that the energy in the MEAM is composed of two terms, the embedding function term and the pair interaction term.

The embedding function is given in the following form [16],

$$F(\overline{\rho}) = AE_c \frac{\overline{\rho}}{\overline{\rho}^o} \ln \frac{\overline{\rho}}{\overline{\rho}^o} \tag{A.1}$$

where A is an adjustable parameter, E_c is the cohesive energy and $\overline{\rho}^o$ is the background electron density for a reference structure. The reference structure is a structure where individual atoms are on the exact lattice points. Normally, the equilibrium structure is taken as the reference structure for elements. The background electron density $\overline{\rho}_i$ is composed of spherically symmetric partial electron density, $\rho_i^{(0)}$, and angular contributions, $\rho_i^{(1)}$, $\rho_i^{(2)}$, $\rho_i^{(3)}$. Each partial electron density term has the following form [16,65],

$$(\rho_i^{(0)})^2 = \left[\sum_{j\neq i} S_{ij}\rho_j^{a(0)}(R_{ij})\right]^2 \tag{A.2a}$$

$$(\rho_i^{(1)})^2 = \sum_{\alpha}\left[\sum_{j\neq i} \frac{R_{ij}^{\alpha}}{R_{ij}} S_{ij}\rho_j^{a(1)}(R_{ij})\right]^2 \tag{A.2b}$$

$$(\rho_i^{(2)})^2 = \sum_{\alpha,\beta}\left[\sum_{j\neq i} \frac{R_{ij}^{\alpha}R_{ij}^{\beta}}{R_{ij}^2} S_{ij}\rho_j^{a(2)}(R_{ij})\right]^2 - \frac{1}{3}\left[\sum_{j\neq i} S_{ij}\rho_j^{a(2)}(R_{ij})\right]^2 \tag{A.2c}$$

$$(\rho_i^{(3)})^2 = \sum_{\alpha,\beta,\gamma}\left[\sum_{j\neq i} \frac{R_{ij}^{\alpha}R_{ij}^{\beta}R_{ij}^{\gamma}}{R_{ij}^3} S_{ij}\rho_j^{a(3)}(R_{ij})\right]^2 - \frac{3}{5}\sum_{\alpha}\left[\sum_{j\neq i} \frac{R_{ij}^{\alpha}}{R_{ij}} S_{ij}\rho_j^{a(3)}(R_{ij})\right]^2. \tag{A.2d}$$

Here, $\rho_j^{a(h)}$ represent atomic electron densities from j atom at a distance R_{ij} from site i. R_{ij}^{α} is the α component of the distance vector between atoms j and i ($\alpha = x, y, z$). The expression for $(\rho_i^{(3)})^2$ (Eq. (A.2d)) is that modified later in order to make the partial electron densities orthogonal [65]. The way of combining the partial electron densities to give the total background electron density is not unique, and several expressions have been proposed [27]. Among them, the following form that can be widely used without numerical error is taken in the present work

$$\overline{\rho}_i = \rho_i^{(0)} G(\Gamma) \tag{A.3}$$

where

$$G(\Gamma) = \frac{2}{1+e^{-\Gamma}} \tag{A.4}$$

and

$$\Gamma = \sum_{h=1}^{3} t_i^{(h)} \left[\frac{\rho_i^{(h)}}{\rho_i^{(0)}}\right]^2 \tag{A.5}$$

$t_i^{(h)}$ are adjustable parameters. The atomic electron density is given as,

$$\rho_j^{a(h)}(R) = \rho_0 e^{-\beta^{(h)}(R/r_e - 1)} \tag{A.6}$$

where ρ_0 is a scaling factor, $\beta^{(h)}$ are adjustable parameters and r_e is the nearest-neighbor distance in the equilibrium reference

structure. The scaling factor does not have any effect on calculations for elements, but it can affect the calculations for alloy systems.

In the MEAM no specific functional expression is given directly to $\phi(R)$. Instead, the atomic energy (total energy per atom) is evaluated by some means as a function of nearest-neighbor distance. Then, the value of $\phi(R)$ is computed from known values of the total energy and the embedding energy, as a function of nearest-neighbor distance.

Let's consider a reference structure once again. Here, every atom has the same environment and the same energy. If up to second nearest-neighbor interactions are considered as done in the 2NN MEAM [17,18], the total energy per atom in a reference structure can be written as follows:

$$E^a(R) = F(\overline{\rho}^o(R)) + \frac{Z_1}{2}\phi(R) + \frac{Z_2 S}{2}\phi(aR) \tag{A.7}$$

where Z_1 and Z_2 are the number of first and second nearest-neighbor atoms, respectively. S is the screening factor for second nearest-neighbor interactions (the screening factor for first nearest-neighbor interactions is 1), and a is the ratio between the second and first nearest-neighbor distances. It should be noted that for a given reference structure, S and a are constants, and the total energy and the embedding energy become functions of only nearest-neighbor distance R. On the other hand, the energy per atom for a reference structure can be obtained from the zero-temperature universal equation of state of Rose et al. [26] as a function of nearest-neighbor distance R

$$E^u(R) = -E_c(1 + a^* + da^{*3})e^{-a^*} \tag{A.8}$$

where d is an adjustable parameter, and

$$a^* = \alpha(R/r_e - 1) \tag{A.9}$$

and

$$\alpha = \left(\frac{9B\Omega}{E_c}\right)^{1/2}. \tag{A.10}$$

$E^u(R)$ is the universal function for a uniform expansion or contraction in the reference structure, B is the bulk modulus and Ω is the equilibrium atomic volume.

Basically, the pair potential between two atoms separated by a distance R, $\phi(R)$, can be obtained by equating Eqs. (A.7) and (A.8). However, it is not trivial because Eq. (A.7) contains two pair potential terms. In order to derive an expression for the pair interaction, $\phi(R)$, another pair potential, $\psi(R)$, is introduced:

$$E^u(R) = F(\overline{\rho}^o(R)) + \frac{Z_1}{2}\psi(R) \tag{A.11}$$

where

$$\psi(R) = \phi(R) + \frac{Z_2 S}{Z_1}\phi(aR). \tag{A.12}$$

$\psi(R)$ can be computed from Eq. (A.11) as a function of R, as follows:

$$\psi(R) = \frac{2}{Z_1}[E^u(R) - F(\overline{\rho}^o(R))], \tag{A.13}$$

and the expression for the pair potential $\phi(R)$ is obtained from Eq. (A.12) as follows:

$$\phi(R) = \psi(R) + \sum_{n=1}(-1)^n \left(\frac{Z_2 S}{Z_1}\right)^n \psi(a^n R). \tag{A.14}$$

Here, the summation is performed until a correct value of atomic energy is obtained for the equilibrium reference structure.

It should be noted here that the original first nearest neighbor MEAM is a special case ($S = 0$) of the present 2NN MEAM. In the original MEAM, the neglect of the second nearest-neighbor interactions is made by the use of a strong many-body screening function [27]. In the same way, the consideration of the second nearest-neighbor interactions in the modified formalism is effected by adjusting the many-body screening function so that it becomes less severe. In the MEAM, the many-body screening function between atoms i and j, S_{ij}, is defined as the product of the screening factors, S_{ikj}, due to all other neighbor atoms k:

$$S_{ij} = \prod_{k \neq i,j} S_{ikj}. \tag{A.15}$$

The screening factor S_{ikj} is computed using a simple geometric construction. Imagine an ellipse on an x, y plane, passing through atoms, i, k and j with the x-axis of the ellipse determined by atoms i and j. The equation of the ellipse is given by,

$$x^2 + \frac{1}{C}y^2 = \left(\frac{1}{2}R_{ij}\right)^2. \tag{A.16}$$

For each k atom, the value of parameter C can be computed from relative distances among the three atoms, i, j and k, as follows:

$$C = \frac{2(X_{ik} + X_{kj}) - (X_{ik} - X_{kj})^2 - 1}{1 - (X_{ik} - X_{kj})^2} \tag{A.17}$$

where $X_{ik} = (R_{ik}/R_{ij})^2$ and $X_{kj} = (R_{kj}/R_{ij})^2$. The screening factor, S_{ikj} is defined as a function of C as follows:

$$S_{ikj} = f_c\left[\frac{C - C_{\min}}{C_{\max} - C_{\min}}\right] \tag{A.18}$$

where $C_{\min}$ and $C_{\max}$ are the limiting values of C determining the extent of screening and the smooth cutoff function is

$$\begin{array}{ll} f_c(x) = 1 & x \geq 1 \\ \left[1 - (1-x)^4\right]^2 & 0 < x < 1 \\ 0 & x \leq 0. \end{array} \tag{A.19}$$

The basic idea for the screening is as follows: First, define two limiting values, $C_{\max}$ and $C_{\min}$ ($C_{\max} > C_{\min}$). Then, if the atom k is outside the ellipse defined by $C_{\max}$, it is thought that the atom k does not have any effect on the interaction between atoms i and j. If the atom k is inside the ellipse defined by $C_{\min}$, it is thought that the atom k completely screens the i–j interaction, and between $C_{\max}$ and $C_{\min}$ the screening changes gradually. In the numerical procedure of simulation, the electron density and pair potential are multiplied by the screening function S_{ij}, as is done in Eq. (1) and Eqs. (A.2a)–(A.2d). Therefore, $S_{ij} = 1$ and $S_{ij} = 0$ mean that the interaction between atoms i and j is unscreened and completely screened, respectively. In addition to the many-body screening function, a radial cutoff function, which is given by $f_c[(r_c - r)/\Delta r]$ where r_c is the cutoff distance and Δr (0.1 Å) is the cutoff region, is also applied to the atomic electron density and pair potential [27]. The radial cutoff distance is chosen so that it does not have any effect on the calculation results due to the many-body screening. This is only for computational convenience, that is, to save computation time.

References

[1] M.S. Daw, S.M. Foiles, M.I. Baskes, The embedded-atom method: a review of theory and applications, Mater. Sci. Rep. 9 (1993) 251–310.
[2] B.-J. Lee, A semi-empirical atomistic approach in materials research, J. Phase Equilib. and Diff. 30 (2009) 509–516.
[3] S. Kohlhoff, P. Gumbsch, H.F. Fischmeister, Crack propagation in bcc crystals studied with a combined finite-element and atomistic model, Philos. Mag. A 64 (1991) 851–878.
[4] W.A. Curtin, R.E. Miller, Atomistic/continuum coupling in computational materials science, Model. Simul. Mater. Sci. Eng. 11 (2003) R33–R68.
[5] L.P. Kubin, G. Canova, The modelling of dislocation patterns, Scripta Met. 27 (1992) 957–962.

[6] E. Van der Giessen, A. Needleman, Discrete dislocation plasticity: a simple planar model, Model. Simul. Mater. Sci. Eng. 3 (1995) 689–735.
[7] A.E. Carlsson, in: H. Ehrenreich, D. Turnbull (Eds.), Solid State Physics: Advances in Research and Application, Vol.43, Academic Press, New York, 1990.
[8] M.S. Daw, M.I. Baskes, Embedded-atom method: derivation and application to impurities, surfaces, and other defects in metals, Phys. Rev. B 29 (1984) 6443–6453.
[9] M.W. Finnis, J.E. Sinclair, A simple empirical N-body potential for transition metals, Philos. Mag. A 50 (1984) 45–55.
[10] F. Ercolessi, E. Tosatti, M. Parrinello, Au (100) surface reconstruction, Phys. Rev. Lett. 57 (1986) 719–722.
[11] J. Tersoff, New empirical approach for the structure and energy of covalent systems, Phys. Rev. B 37 (1988) 6991–7000.
[12] V. Rosato, M. Guillope, B. Legrand, Thermodynamical and structural properties of fcc transition metals using a simple tight-binding model, Philos. Mag. A 59 (1989) 321–336.
[13] D.W. Brenner, Empirical potential for hydrocarbons for use in simulating the chemical vapor deposition of diamond films, Phys. Rev. B 42 (1990) 9458–9471.
[14] S.J. Stuart, A.B. Tutein, J.A. Harrison, A reactive potential for hydrocarbons with intermolecular interactions, J. Chem. Phys. 112 (2000) 6472–6486.
[15] A.C.T. van Duin, S. Dasgupta, F. Lorant, W.A. Goddard III, ReaxFF: a reactive force field for hydrocarbons, J. Phys. Chem. A 105 (2001) 9396–9409.
[16] M.I. Baskes, Modified embedded-atom method potentials for cubic materials and impurities, Phys. Rev. B 46 (1992) 2727–2742.
[17] B.-J. Lee, M.I. Baskes, Second nearest-neighbor modified embedded-atom method potential, Phys. Rev. B 62 (2000) 8564–8567.
[18] B.-J. Lee, M.I. Baskes, H. Kim, Y.K. Cho, Second nearest-neighbor modified embedded atom method potentials for BCC transition metals, Phys. Rev. B 64 (2001) 184102.
[19] B.-J. Lee, J.-H. Shim, M.I. Baskes, Semi-empirical atomic potentials for the FCC Metals Cu, Ag, Au, Ni, Pd, Pt, Al and Pb based on first and second nearest-neighbor modified embedded atom method, Phys. Rev. B 68 (2003) 144112.
[20] Y.-M. Kim, B.-J. Lee, M.I. Baskes, Modified embedded atom method interatomic potentials for Ti and Zr, Phys. Rev. B 74 (2006) 014101.
[21] Y.-M. Kim, N.J. Kim, B.-J. Lee, Atomistic modeling of pure Mg and Mg–Al system, CALPHAD 33 (2009) 650–657.
[22] Y.-M. Kim, Y.-H. Shin, B.-J. Lee, Modified embedded-atom method interatomic potentials for pure Mn and Fe–Mn System, Acta Mater. 57 (2009) 474–482.
[23] B.-J. Lee, J.W. Lee, A modified embedded atom method interatomic potential for carbon, CALPHAD 29 (2005) 7–16.
[24] B.-J. Lee, A modified embedded atom method interatomic potential for silicon, CALPHAD 31 (2007) 95–104.
[25] E.H. Kim, Y.-H. Shin, B.-J. Lee, A modified embedded atom method interatomic potential for germanium, CALPHAD 32 (2008) 34–42.
[26] J.H. Rose, J.R. Smith, F. Guinea, J. Ferrante, Universal features of the equation of state of metals, Phys. Rev. B 29 (1984) 2963–2969.
[27] M.I. Baskes, Determination of modified embedded atom method parameters for nickel, Mater. Chem. Phys. 50 (1997) 152–158.
[28] B.-J. Lee, T.-H. Lee, S.-J. Kim, A modified embedded-atom method interatomic potential for the Fe–N System: a comparative study with the Fe–C system, Acta Mater. 54 (2006) 4597–4607.
[29] H.-K. Kim, W.-S. Jung, B.-J. Lee, Modified embedded-atom method interatomic potentials for the Fe–Ti–C and Fe–Ti–N systems, Acta Mater. 57 (2009) 3140–3147.
[30] B.-J. Lee, A modified embedded atom method interatomic potential for the Fe–C system, Acta Mater. 54 (2006) 701–711.
[31] Y.-M. Kim, B.-J. Lee, Modified embedded-atom method interatomic potentials for the Ti–C and Ti–N systems, Acta Mater. 56 (2008) 3481–3489.
[32] I. Sa, B.-J. Lee, Modified embedded-atom method interatomic potentials for the Fe–Nb and Fe–Ti systems, Scripta Mater. 59 (2008) 595–598.
[33] H.-K. Kim, W.-S. Jung, B.-J. Lee, Modified embedded-atom method interatomic potentials for the Nb–C, Nb–N, Fe–Nb–C and Fe–Nb–N systems, J. Mater. Res. 25 (2010) 1288–1297.
[34] B.E. Sundquist, A direct determination of the anisotropy of the surface free energy of solid gold, silver, copper, nickel, and alpha and gamma iron, Acta Metall. 12 (1964) 67–86.
[35] H.E. Grenga, R. Kumar, Surface energy anisotropy of iron, Surf. Sci. 61 (1976) 283–290.
[36] E.C. Do, Y.-H. Shin, B.-J. Lee, A modified embedded atom method interatomic potential for indium, CALPHAD 32 (2008) 82–88.
[37] B.-J. Lee, Pohang University of Science and Technology (POSTECH), Korea, unpublished work.
[38] B.-J. Lee, J.-W. Jang, A modified embedded-atom method interatomic potential for the Fe–H system, Acta Mater. 55 (2007) 6779–6788.
[39] J.-H. Shim, Korea Institute of Science and Technology (KIST), Korea, unpublished work.
[40] E. Lee, B.-J. Lee, Modified embedded-atom method interatomic potential for the Fe–Al system, J. Phys.: Condens. Matter 22 (2010) 175702.
[41] B.-J. Lee, J.-H. Shim, H.M. Park, A semi-empirical atomic potential for the Fe–Cr binary system, CALPHAD 25 (2001) 527–534.
[42] B.-J. Lee, B.D. Wirth, J.-H. Shim, J. Kwon, S.C. Kwon, J.-H. Hong, An MEAM interatomic potential for the Fe–Cu alloy system and cascade simulation on pure Fe and Fe–Cu alloy, Phys. Rev. B 71 (2005) 184205.
[43] J. Kim, Y. Koo, B.-J. Lee, Modified embedded-atom method interatomic potential for the Fe–Pt alloy system, J. Mater. Res. 21 (2006) 199–208.
[44] K.-H. Kang, I. Sa, J.-C. Lee, E. Fleury, B.-J. Lee, An atomistic modeling of the Cu–Zr–Ag bulk metallic glass system, Scripta Mater. 61 (2009) 801–804.
[45] J. Agren, M.T. Clavaguera-Mora, A. Costa e Silva, D. Djurovic, T. Gomez-Acebo, B.-J. Lee, Z.-K. Liu, P. Miodownik, H. Seifert, Applications of computational thermodynamics — the extension from phase equilibrium to phase transformations and other properties, CALPHAD 31 (2007) 53–74.
[46] B.-J. Lee, J.-H. Shim, A modified embedded atom method interatomic potential for the Cu–Ni System, CALPHAD 28 (2004) 125–132.
[47] Y.-M. Kim, B.-J. Lee, A semi-empirical interatomic potential for the Cu–Ti binary system, Mater. Sci. Eng. A (2007) 449–451. 733–736.
[48] Y.-M. Kim, B.-J. Lee, A modified embedded-atom method interatomic potential for the Cu–Zr system, J. Mater. Res. 23 (2008) 1095–1104.
[49] J.-H. Shim, S.I. Park, Y.W. Cho, B.-J. Lee, Modified embedded-atom method calculation for the Ni–W system, J. Mater. Res. 18 (2003) 1863–1867.
[50] E.C. Do, Y.-H. Shin, B.-J. Lee, Atomistic modeling of III-V nitrides: modified embedded-atom method interatomic potentials for GaN, InN and $Ga_{1-x}In_xN$, J. Phys.: Condens. Matter 21 (2009) 325801.
[51] V.G. Gavriljuk, H. Berns, High Nitrogen Steels: Structure, Properties, Manufacture, Applications, Springer, Berlin, 1999.
[52] J. Schiøtz, F.D. Di Tolla, K.W. Jacobsen, Softening of nanocrystalline metals at very small grain sizes, Nature 391 (1998) 561–563.
[53] S.G. Kim, Kunsan National University, country-regionKorea, unpublished work.
[54] H.-K. Kim, W.-S. Ko, H.-J. Lee, S.G. Kim, B.-J. Lee, An identification scheme of grain boundaries and construction of grain boundary energy database (2010) (submitted for publication).
[55] B.-J. Lee, S.-H. Choi, Computation of grain boundary energies, Model. Simul. Mater. Sci. Eng. 42 (2004) 621–632.
[56] M. Wen, X.-J. Xu, S. Fukuyama, K. Yokogawa, Embedded-atom-method functions for the body-centered-cubic iron and hydrogen, J. Mater. Res. 16 (2001) 3496–3502.
[57] M.I. Baskes, R.A. Johnson, Modified embedded atom potentials for HCP metals, Model. Simul. Mater. Sci. Eng. 2 (1994) 147–163.
[58] S. Kerisit, N. Aaron Deskins, K.M. Rosso, M. Dupuis, A shell model for atomistic simulation of charge transfer in titania, J. Phys. Chem. C 112 (2008) 7678–7688.
[59] J.D. Gale, A.L. Rohl, The general utility lattice program (GULP), Molecular Simul. 29 (2003) 291–341.
[60] A.C.T. van Duin, A. Strachan, S. Stewman, Q. Zhang, X. Xu, W.A. Goddard III, ReaxFFSiO reactive force field for silicon and silicon oxide systems, J. Phys. Chem. A 107 (2003) 3803–3811.
[61] J. Yu, S.B. Sinnott, S.R. Phillpot, Charge optimized many-body potential for the Si/SiO_2 system, Phy. Rev. B 75 (2007) 085311.
[62] M.I. Baskes, Modified Embedded Atom Method Calculations of Interfaces, Report number: SAND–96-8484C, Sandia National Laboratories, Livermore, 1996.
[63] S.L. Dudarev, P.M. Derlet, A 'Magnetic' interatomic potential for molecular dynamics simulations, J. Phys.: Condens. Matter 17 (2005) 7097–7118.
[64] M. Müller, P. Erhart, K. Albe, Analytic bond-order potential for BCC and FCC iron—comparison with established embedded-atom method potentials, J. Phys.: Condens. Matter 19 (2007) 326220.
[65] M.I. Baskes, Atomic potentials for the molybdenum–silicon system, Mater. Sci. Eng. A 261 (1999) 165–168.